Purdue University
Purdue e-Pubs

International Compressor Engineering Conference

School of Mechanical Engineering

2006

Transient Thermal Analysis of Screw Compressors, Part II: Transient Thermal Analysis of a Screw Compressor to Determine Rotor-to-Housing Clearances

Bob Weathers
Trane

Jack Sauls
Trane

Gordon Powell
Trane

Transient Thermal Analysis of Screw Compressors, Part II Transient Thermal Analysis of a Screw Compressor to Determine Rotor-to-Housing Clearances

Bob WEATHERS
Phone: 608-787-2729; FAX: 608-787-2669
Email: bweathers@trane.com

Jack SAULS
Phone: 608-787-2517; FAX: 608-787-2669
Email: jsauls@trane.com

Gordon POWELL
Phone: 608-787-4386; FAX: 608-787-2669
Email: gpowell@trane.com

Trane
Compressor Development and Technology
3600 Pammel Creek Road; La Crosse, WI 54601 USA

ABSTRACT

This paper is the second of a three part report on the transient thermal analysis of screw compressors. As noted in Part I, clearances between rotating and stationary parts of a screw compressor directly influence compressor performance and reliability. While tight clearances lead to higher performance, catastrophic failure can result if clearances are too tight and rotors contact the housing. The design goal is to select clearances tight enough for high performance but not so tight that "rotor rubs" occur and product reliability becomes an issue. The analytical tool described here gives insight into how the various clearances change during compressor operation. Armed with this knowledge, the designer can explore different concepts that ultimately lead to a more reliable, robust, and energy efficient compressor.

In this part of the report, an analytical method is described that uses the calculated heat transfer coefficients and bulk temperatures from Part I. After applying these thermal boundary conditions, transient metal temperatures are predicted throughout the compressor. Next, the predicted metal temperatures are compared to experiment. Finally, changes in rotor-to-housing clearances caused by thermal transients are quantified and discussed.

1. INTRODUCTION

As noted in Part I, an understanding of how clearances change during compressor operation is needed so they can be better managed. High efficiency requires tight clearances. But if clearances are too tight, "rubs" occur and product reliability becomes an issue. A complicating factor in managing these clearances is that they change during normal operation.

"Cold" clearances describe the situation when all compressor parts are at ambient temperature. Once a steady state condition is achieved, temperatures vary from roughly ambient on the outside of the compressor to 150 degrees or more at discharge. Because temperatures of the various compressor components are no longer uniform, they have now taken a new size and shape. This, in turn, means the clearance between the various parts is different than their "cold" value.

Three factors combine to cause temperatures (and hence clearances) to change in a non-uniform way during transient events (e.g., compressor start up or changing the set point).

- Refrigerant heat transfer coefficients, bulk temperatures, and pressures vary spatially throughout the compressor as well as with time.

- Thermal inertia of the various compressor parts differ due to their different mass. This means different parts absorb heat at different rates. They will not march toward their new steady state temperature at the same rate.
- If different materials are used, material property differences also affect thermal inertia and rate of thermal growth.

This paper describes a modeling approach used to study these changes in clearance. Experimentally measured temperatures are compared to analytical predictions. Finally, changes in rotor-to-housing clearances caused by thermal transients are quantified and discussed.

2. MODELING APPROACH

2.1 Modeling Overview

The general approach is to first solve the convective heat transfer problem for the compressor to calculate metal temperatures. Once metal temperatures are available, the thermal growth problem is solved and clearances calculated.

Figure 1 shows an external view of the screw compressor model while Figure 2 shows an internal view with the top half removed. Being able to easily remove the top half and "look inside" proved to be a very efficient way of presenting results.

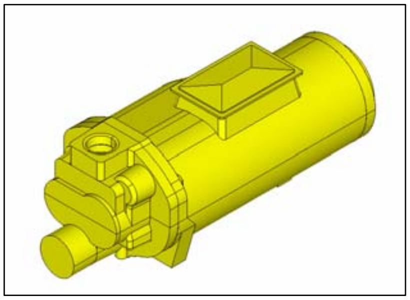

Figure 1 Screw Compressor - External

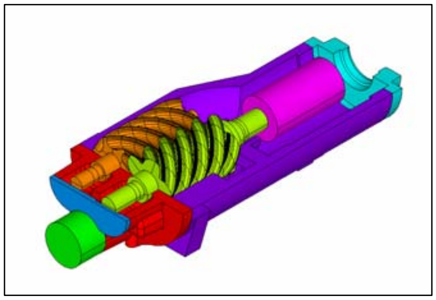

Figure 2 Screw Compressor - Internal

Care was taken in the construction of the models of the screw rotors and shafts. A generic scheme was developed that allows the user to create the screw rotors and shafts by reading a geometry file in a standard format. The geometry file contains information about points on the rotor profile, rotor lead and length, shaft dimensions, and bearing locations. Given this information, a hex dominant mesh is created such as the one in Figure 3. The technique creates the male and female shafts and then correctly positions them in the model. This scheme makes it possible to more easily explore how different shaft and rotor geometries impact clearance and rotor meshing.

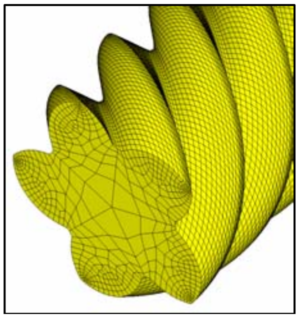

Figure 3 Hex Dominant Rotor Mesh

Having quads on the surface of the screw rotors allows predicted rotor displacements to be organized in a very efficient way. It is much more difficult to organize this information using a triangular surface mesh. Displacements caused by thermal growth are needed for subsequent rotor-to-rotor clearance calculations discussed in Part III of this series.

In the preliminary modeling stage, a technique was also developed for applying the different heat transfer coefficients calculated in Part I. For example, areas where heat transfer parameters for a vertical flat plate are appropriate have an area attribute of 1, horizontal flat plates 2, oil passages 3, and so on. Since these heat transfer values are related to areas rather than the underlying mesh, the model can be re-meshed as needed and boundary conditions re-applied with relative ease.

2.2 Applying Heat Transfer Coefficients and Bulk Temperatures to the Rotor Bore

While the rotor bores followed the protocol of being "categorized" using a unique area attribute, other details of applying heat transfer to them is more complicated and needs additional explanation. Since the same procedure is used for both male and female rotor bore, only the male will be described.

After the male rotor bore surface is assigned a unique area attribute, a very fine area mesh is created on the surface. Node locations on this surface are written out as theta-z locations. Since the radius is constant, only theta and z are needed to uniquely identify a location on the bore surface. With node locations in-hand, the technique described by Sauls in Section 2.1 of Part I of this series is used to calculate the heat transfer coefficient and bulk temperature at each node location once and for all. This information is passed back to the FE model in a file that contains the predicted heat transfer performance at each node.

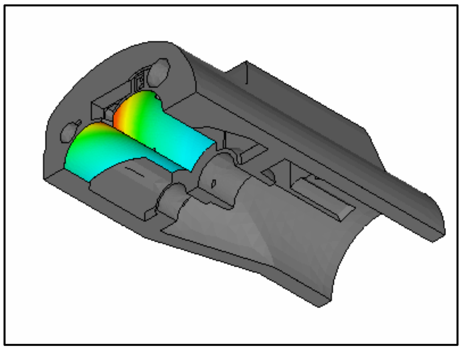

Figure 4 Rotor Bore Heat Transfer

The rotor housing is then more coarsely meshed in preparation for the thermal analysis. After the housing is meshed, heat transfer information is mapped from the very fine mesh onto the mesh at hand. This approach allows the rotor housing to be re-meshed as necessary without having to create a new set of heat transfer coefficients and bulk temperatures. Heat transfer information generated early on in the process can be used over and over.

Figure 4 shows heat transfer coefficients mapped onto the rotor bore. Bulk temperature plots are qualitatively identical. Highest value is in red. For clarity, coefficients not on the bore are grayed out.

2.3 Applying Heat Transfer Coefficients and Bulk Temperatures to the Screw Rotors

Heat transfer boundary conditions are applied to the screw rotors in much the same way as they are to the rotor bores. Again, though, there are a few differences worthy of further explanation. And, as with the bores, since the same procedure is used for both male and female rotors, only the male will be discussed.

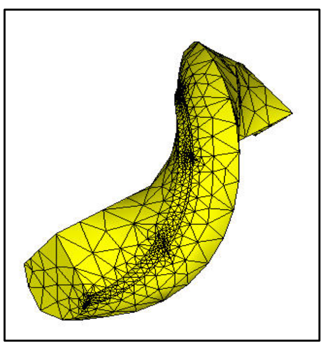

Figure 5 Triangular Mesh

The male screw rotor surface is first assigned a unique area attribute so it can be easily selected.

Section 2.1 of this paper points out that a hex mesh is used on the surface of the screw rotors rather than a triangular one. Figure 5 shows what a single lobe would look like if it had a triangular mesh on its surface rather than rectangles. Note that nodes are "sprinkled" on the surface. This irregular node pattern does not lend itself to an efficient exchange of information with other programs.

Figure 6 continues the comparison and shows how easily a rectangular surface mesh can be unwrapped onto a 2-D surface. For reference, a red rectangle is shown that has been mapped from the meshed lobe onto the unwrapped 2-D surface. It should now be obvious that the rectangular mesh offers the advantage of being able to uniquely identify each node location in a well organized table. The table has axial locations as rows while columns are distance along the rotor profile. Each surface node maps nicely into a particular row and column. While a triangular surface mesh can still exchange the necessary information, it cannot be as easily organized.

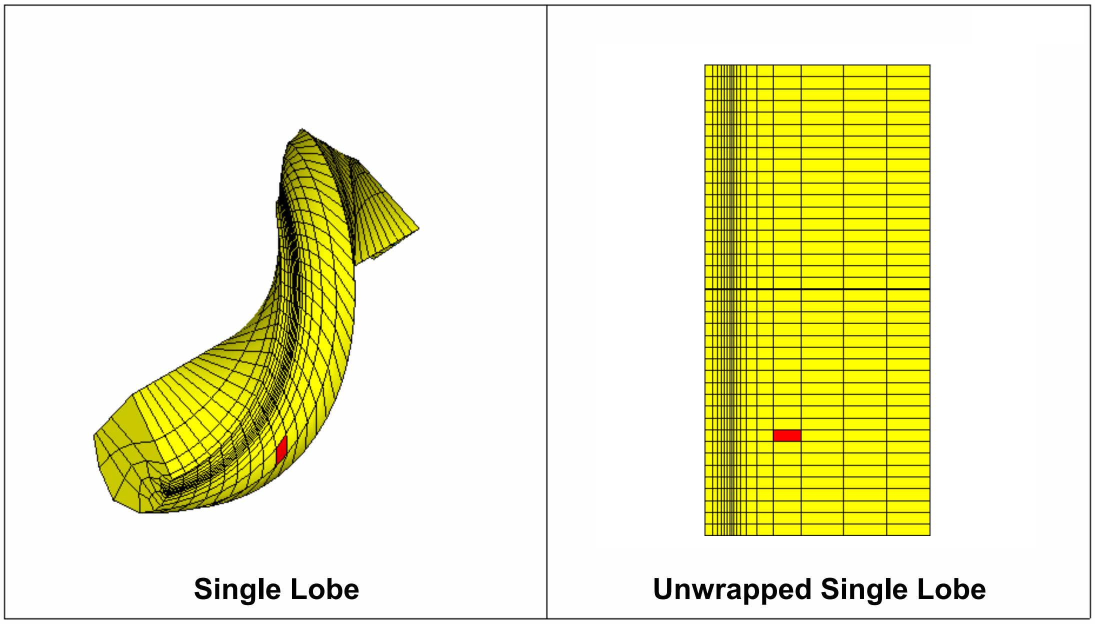

Figure 6 Rectangular Surface Mesh

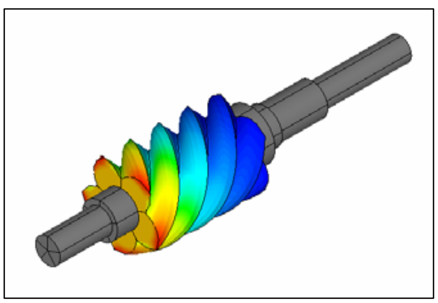

Figure 7 Male Rotor Bulk Temperatures

Once the convention was established for describing node locations on the screw rotors, the process proceeds exactly as it did for the rotor bores. A fine rectangular mesh is created on the surface and passed to the technique described by Sauls in Section 2.2 of Part I of this series. Predicted nodal heat transfer performance is then passed back to the FE model. The heat transfer information from the fine area mesh is mapped onto the screw rotors and can be re-used if the rotors are ever re-meshed.

Figure 7 shows the bulk temperatures mapped onto the screw rotors. Again for clarity, shaft bulk temperatures are grayed out. Highest temperature is in red and lowest in blue

2.4 Applying Heat Transfer to the Bearing and Rotor Housing Faces

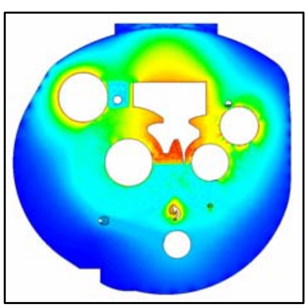

Figure 8 Bearing Head Bulk Temperatures

Figure 8 shows refrigerant bulk temperatures mapped onto the bearing head. As before, node locations are exported to an external program where heat transfer values are calculated.

Hottest temperature is in red and coldest in blue. A heat transfer coefficient plot is qualitatively similar. Note that bulk temperatures change abruptly along a horizontal line joining the male and female bore centerlines. Suction conditions prevail below this line and discharge conditions dominate above it.

A similar approach is used for the face of the rotor housing.

2.5 Flanges, Bearings, and Shafts

Flanges are modeled as if the major castings are welded together from the bolt centerline to the flange OD. Hence, for the thermal analysis, heat can be conducted from one housing to its neighbor without introducing any additional thermal resistance. An adiabatic condition is specified at the suction inlet pipe flange. For the subsequent displacement solution, nodes from the bolt circle to flange OD on each side of a flange move in tandem.

No exchange of heat occurs between the shafts and housings. For the displacement solution, shafts are tied axially to the compressor housing at the center of the thrust bearing via constraint equations. Constraint equations are also used to keep shafts centered in the deformed bearing bores. Shaft axial motion is permitted in the radial bearings.

3. SOLUTION

3.1 Thermal Analysis

The thermal analysis proceeds in a straightforward fashion. Either a steady state or a transient thermal problem is solved. Radiation is neglected. In the case of a transient solution, heat transfer coefficients and bulk temperatures are updated each time step. "Sanity checks" are made to insure that the metal temperatures from the transient thermal analysis approach the steady state solution.

3.2 Displacement Solution

Metal temperatures predicted by the thermal analysis are used as a thermal boundary condition for the displacement solution. Gravity, rotary inertia of the spinning parts, and internal pressure are neglected. Rigid body motion is prevented by constraining a few nodes on the feet of the compressor.

4. RESULTS

4.1 Analytical Thermal Results

Figure 9 shows predicted metal temperatures at two different times in the thermal analysis. The same temperature scale is used in both plots with the hottest metal temperature shown in red. The left picture plots metal temperatures early in a start up transient while the right shows temperatures much later in the start up cycle.

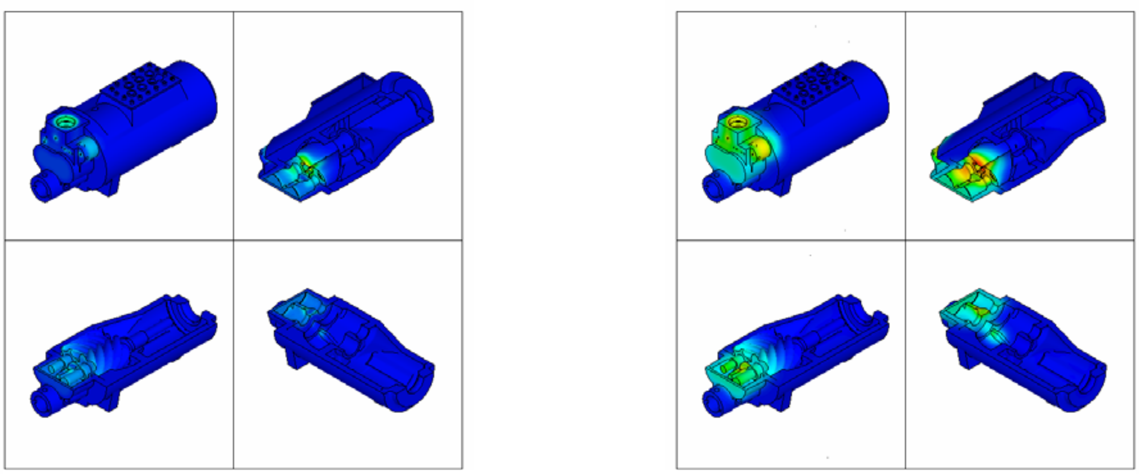

Early In The Start Cycle　　　　Late In The Start Cycle

Figure 9 Metal Temperatures at Two Different Times In a Transient Start

These metal temperatures at different time steps are then used as boundary conditions for the displacement solution. Other displacement solution details and boundary conditions are described in Sections 2.5 and 3.2.

4.2 Comparison Between Predicted and Measured Metal Temperatures

Twenty-two thermocouples were placed inside an experimental compressor and temperatures measured during compressor start-up. Analytically predicted temperatures were then plotted in Excel and compared to the measured ones. While the agreement between analysis and experiment was surprisingly good (usually less than 5 degs F) at most locations, a few of the results suggested changes that could be made to the thermal boundary conditions to improve agreement.

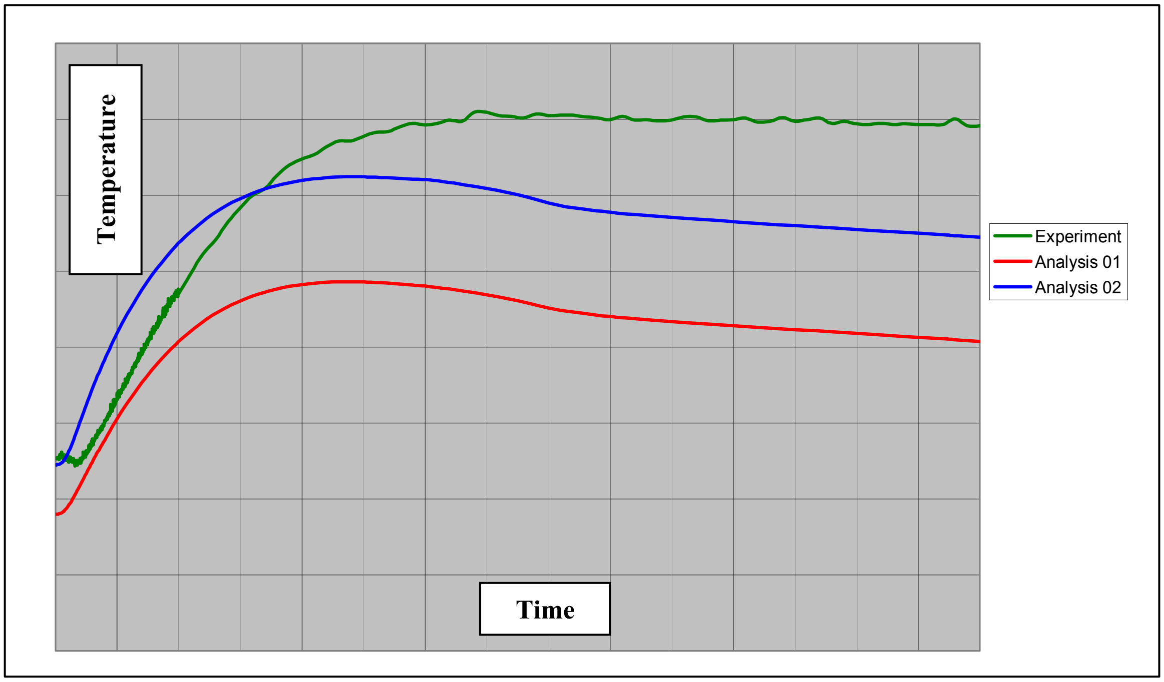

Figure 10 Experiment vs. Analysis, Male Shaft Centerline Temperature At Discharge End

Figure 10 compares analytical and experimental temperatures at a point on the male shaft centerline at the discharge end. Experimental results are shown in green. Red "Analysis 01" is the first modeling attempt. After reviewing these results, it was concluded that the analysis might be improved if heat generated by the seals at the discharge end were added. It also appeared the assumed bulk temperatures around the shaft at the discharge end had been underestimated. And temperature measurements of the oil at the discharge end showed that it too had been underestimated. Adjustments were made and the thermal analysis re-run. Blue "Analysis 02" is the result of this second run. The modeling error was cut in half.

4.3 Change In Rotor-to-Housing Clearances During Start Up

Figure 11 shows the predicted change in clearance between the screw rotor and rotor bore at two different times during the start cycle. Red reflects regions where the clearance is smallest while blue shows where it's largest.

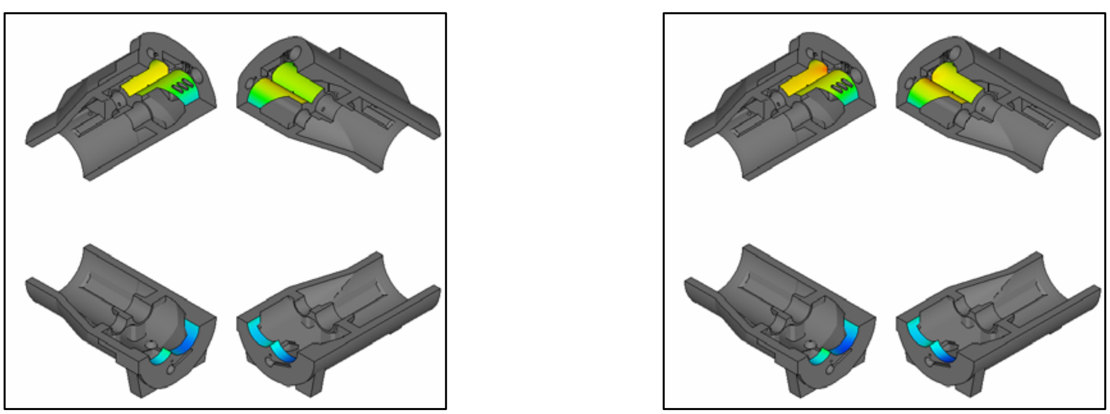

Early In The Start Cycle — Late In The Start Cycle

Figure 11 Predicted Clearance Between Screw Rotor And Rotor Bore

Although clearances were not experimentally measured, laboratory results provide anecdotal evidence that rubs tend to occur in the same areas where analysis predicts clearances are the smallest.

4.4 Change In End Clearances During Start Up

Figure 12 shows the predicted change in clearance between the discharge end of the screw rotor and the face of the bearing housing at two different times during the start cycle. Red reflects regions where the clearance is the smallest while blue shows where it's largest. Regions not in the "shadow" of the rotors have been grayed out.

As was the case with rotor clearances, anecdotal laboratory results show that rubs tend to occur in the same areas where analysis predicts the clearances are smallest.

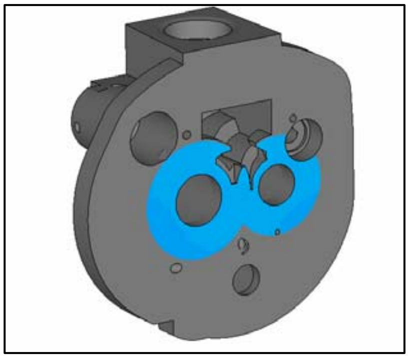

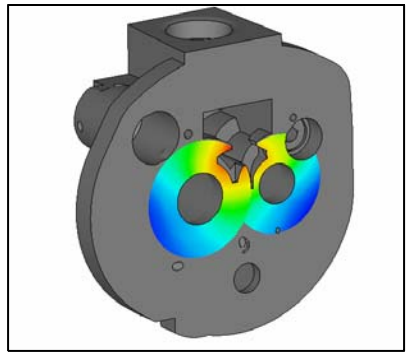

Early In The Start Cycle　　　　Late in The Start Cycle

Figure 12 Predicted Clearance Between Screw Rotors And Bearing Head

4.5 Plot of Transient Change In End Clearances During Start Up

Figure 13 shows how the end clearance on the male rotor changes during start up. At time 0, the faces of the screw rotors are a uniform distance away from the face of the bearing housing. Once the compressor is started, the

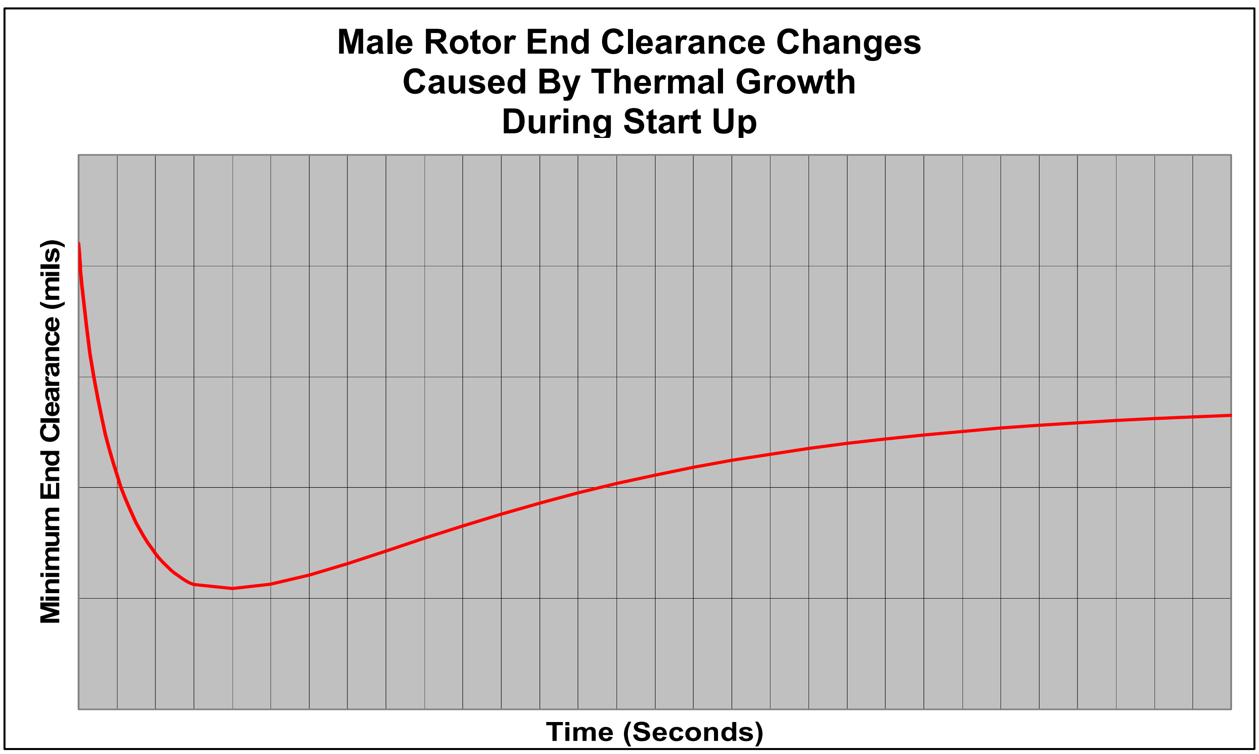

Figure 13 Change In Male Rotor End Clearance During Start Up

different parts change size in different ways as a result of the spatially varying heat transfer. Differences in thermal inertia of the various parts also cause the components to change size at different rates. This, in turn, means that the clearances between the various components change in a non-uniform way as a function of time. Figure 13 was generated by searching for the minimum clearance between the discharge face of the spinning male rotor and its "shadow" on the face of the bearing housing. This minimum clearance will not occur at the same location at each time step.

5. CONCLUSIONS

A semi-automatic method has been developed to study how clearances change during transient operation of a screw compressor. The technique has been shown capable of predicting experimentally measured temperatures with reasonable accuracy. Although operating clearances were not measured, anecdotal laboratory evidence shows that rubs occur in the same general area where this analysis predicts clearances are a minimum in transient operation.

The significant benefit of this combined work is the insight it provides into how clearances change during transient operation. Once steady state is achieved, clearances are often little changed from their values in their cold "as assembled" state. However, large excursions from these "as assembled" clearances are predicted during transient operation. This phenomenon is driven by the variations in thermal inertias of rotors and housings where the thermal inertia mismatch leads to different rates of thermal expansion of the various parts. And this non-uniform growth rate ultimately leads to time varying clearance changes.

REFERENCES

Sauls, J., Powell, G. and Weathers, B., 2006, Transient Thermal Analysis of Screw Compressors, Part I -- Use of Thermodynamic Simulation to Determine Boundary Conditions for Finite Element Analyses, *Proceedings of the 2006 International Engineering Conference at Purdue*, Purdue University.

Powell, G., Weathers, B. and Sauls, J., 2006, Transient Thermal Analysis of Screw Compressors, Part III -- Transient Thermal Analysis of a Screw Compressor to Determine Rotor-to-Rotor Clearances, *Proceedings of the 2006 International Engineering Conference at Purdue*, Purdue University.

Kauder, K. and Keller, G., 1995, Wärmeübergangsrandbedingunen für Schraubenmaschinen, *Schraubenmaschinen – Forschunsberichte des FG Fluidenergiemaschinen Nr. 13*, Universität Dortmund: 5-19.

Kauder, K., Janicki, M. and von Unwerth, T., 2001, Workshop: Simulation of screw-type machines, *Private communication*, University of Dortmund.

ACKNOWLEDGEMENTS

I would like to thank Trane for the opportunity to present the work reported here. And my thanks to Prof. Dr.-Ing. Knut Kauder, Dipl.-Ing. Magnus Janicki and Dr.-Ing. Thomas von Unwerth for their work in this area and their invaluable advice in adapting their results to the application in refrigeration compressors.

And special thanks to my co-authors for their support, advice, and constructive criticism. They are talented engineers and good friends.